



Original Article

# Effect of Electron-impurity Interaction on the Optical Absorption in A Quasi-one-dimensional Electron System

Nguyen Ngoc Thuy Linh<sup>1</sup>, Nguyen Ngoc Hieu<sup>2</sup>,  
Nguyen Thi Nam<sup>3</sup>, Tran Cong Phong<sup>1,\*</sup>

<sup>1</sup>University of Education, Hue University, 34 Le Loi, Hue City, Vietnam

<sup>2</sup>Duy Tan University, 03 Quang Trung, Hai Chau, Da Nang, Vietnam

<sup>3</sup>Hanoi University of Civil Engineering, 55 Giai Phong, Dong Tam, Hai Ba Trung, Hanoi, Vietnam

Received 14 December 2022

Revised 05 February 2023; Accepted 06 February 2023

**Abstract:** In this work, we investigated the optical absorption in a quasi-one-dimensional system subjected to an external electromagnetic wave. The optical absorption coefficient was calculated by using the perturbation theory taking account of the effect of the electron - impurity interaction. The numerical result for the GaAs/AlAs cylindrical semiconductor quantum wire showed the presence of the resonant absorption peaks. The full width at half maximum (FWHM) decreased with increasing the wire radius and increases with increasing temperature. In particular, in the limit of large wire radius, the contribution of transitions between electronic subbands to the absorption spectrum becomes identical, meaning that the system tends to behave as a bulk (three-dimensional) system when the confinement length is large. The obtained results are of significance for further studies and applications of the low dimensional systems in nano-optoelectronic devices.

**Keywords:** One-dimensional system; cylindrical quantum wire; optical absorption; absorption coefficient; electron – impurity interaction.

## 1. Introduction

Quantum wire is a typical structure of the quasi-one-dimensional system which is expected to exhibit extremely high electron mobilities at low temperatures [1]. Physically, the energy levels of the electron in the quantum wire are discrete, and the two-dimensional quantization limits the electron movement.

\* Corresponding author.

E-mail address: [tcphong.sp@hueuni.edu.vn](mailto:tcphong.sp@hueuni.edu.vn)

<https://doi.org/10.25073/2588-1124/vnumap.4796>

Therefore, quantum wire has received much research attention because of such advantages that three-dimensional crystal structures do not have. Besides, optical properties, specifically the absorption of electromagnetic waves of low-dimensional semiconductor systems have also attracted researchers theoretically and experimentally. When there is an additional electromagnetic wave propagating in the material and under the influence of electron - impurity scattering, one can observe some effects such as electron - impurity resonance, electron - impurity resonance detected by optics [2].

In this work, we investigate the optical properties in a cylindrical quantum wire (CQW) placed in a strong electromagnetic wave considering the influence of electron-impurity interactions. The expression of the optical absorption coefficient is explicitly calculated using the perturbation theory. The analytical results are numerically calculated with specific parameters to show the dependence of the absorption coefficient on the photon energy, wire's radius, and temperature. The paper has the following structure: In Section 2, we introduce the expression of the optical absorption coefficient in the CQW under the influence of electron – impurity scattering. The numerical results and discussion for the special GaAs/AlAs CQW are presented in Section 3. Finally, important conclusions are listed in Section 4.

## 2. Analytic Expression for the AC in CQW

We consider a CQW of GaAs with radius  $R$  and length  $L_z$  ( $L_z \gg R$ ), surrounded by the AlAs barrier whose band gap is larger than that of GaAs. When the wire radius is in the order of the electron de Broglie wavelength, quantization effects are important. We choose the cylindrical coordinate system  $(r, \varphi, z)$  so that the axis of the wire points along the  $z$  axis. Under the infinitely deep well approximation, electron wave function and the corresponding energies can be written as [3]:

$$\psi_{n,\ell,k_z}(r, \varphi, z) = \frac{1}{\sqrt{L_z}} e^{ik_z z} e^{in\varphi} C_{n,\ell}(r) J_n \left( B_{n,\ell} \frac{r}{R} \right), \tag{1}$$

$$E_{n,\ell,k_z} = \frac{\hbar^2 k_z^2}{2m_e} + \frac{\hbar^2 B_{n,\ell}^2}{2m_e R^2}, \tag{2}$$

where  $n = 0, \pm 1, \pm 2, \dots$ ;  $\ell = 0, 1, 2, \dots$ ;  $k_z$  denotes the axial wave-vector component;  $C_{n,\ell} = 1/(\sqrt{\pi} y_{n,\ell} R)$  is the normalization factor;  $B_{n,\ell}$  is the  $\ell$ th zero of the  $n$ th order Bessel function;  $y_{n,\ell} = J_{n+1}(B_{n,\ell})$ ,  $m_e$  is the effective mass of electron.

The quantum wire is now stimulated by an optical field characterized by a time-dependent electric field of the form  $E(t) = E_0 \sin \omega t$ , where  $E_0$  and  $\omega$  are the amplitude and frequency of the field, respectively. Electrons in the wire are excited and their interactions with electromagnetic wave photons as well as other particles in the material (impurities, phonons, lattice defects) cause their transitions between electronic states. The absorption coefficient ( $\Gamma$ ) of optical field is related to the state transition probability ( $W_i$ ) by the expression [4]:

$$\Gamma = \frac{\sqrt{\epsilon_r}}{c N_f} \sum_i f_i W_i, \tag{3}$$

where  $c$  is speed of light in vacuum,  $f_i$  is the electron distribution function in the initial state,  $\epsilon_r$  is the dielectric constant of the material, and  $N_f$  is the number of photons with energy  $\hbar\omega$ . According to the second-order Born approximation, the state transition probability of the electron has the form [5]:

$$W_i = \frac{2\pi}{\hbar} \sum_f |\langle f|M|i \rangle|^2 \delta(E_f - E_i - \hbar\omega), \tag{4}$$

where  $\langle f|M|i \rangle$  is the transition matrix element due to electron - photon - impurity interaction. The summation runs over all the possible final states. Combined with the argument of the Delta function, one can write out the transition matrix element as

$$\langle f|M|i\rangle = \sum_{\alpha} \left( \frac{\langle n',\ell',k'_z|-f|H_r|n'',\ell'',k''_z,0\rangle\langle n'',\ell'',k''_z|V_s|n,\ell,k_z\rangle}{E_{n',\ell',k'_z}-E_{n'',\ell'',k''_z}-\hbar\omega} + \frac{\langle n',\ell',k'_z|V_s|n'',\ell'',k''_z\rangle\langle n'',\ell'',k''_z,-f|H_r|n,\ell,k_z,0\rangle}{E_{n,\ell,k_z}-E_{n'',\ell'',k''_z}-\hbar\omega} \right). \quad (5)$$

Here,  $H_r, V_s$  are, respectively, the electron – photon interacting Hamiltonian and the screened potential of ionized impurities which have the forms as given in [5-7]. Performing the straight-forward calculation of the expressions of the transition matrix elements due to electron-photon interaction and electron-impurity scattering, we obtain the expression of the optical absorption coefficient in the cylindrical quantum wire as

$$\Gamma = \frac{2n_i\sqrt{\epsilon_r}U_0^2e^2V}{\gamma\epsilon c(2\pi)^2\hbar^3\omega^3m_e^2(k_B T)^2} \sum_{n,\ell,\ell'} F_{n,\ell,n,\ell'}(R) e^{-\left(\frac{\hbar^2 B_{n,\ell}^2}{2m_e R^2 k_B T}\right)} \times \left[ \hbar\omega - \frac{\hbar^2}{2m_e R^2} (B_{n,\ell'}^2 - B_{n,\ell}^2) \right] \exp \left[ \frac{1}{2k_B T} \left( \hbar\omega - \frac{\hbar^2}{2m_e R^2} (B_{n,\ell'}^2 - B_{n,\ell}^2) \right) \right] \times K_1 \left( \frac{1}{2k_B T} \left( \hbar\omega - \frac{\hbar^2}{2m_e R^2} (B_{n,\ell'}^2 - B_{n,\ell}^2) \right) \right), \quad (6)$$

where  $K_1(x)$  is the modified Bessel function,  $n_i$  is the concentration of impurities,  $F_{n,\ell,n',\ell'}(R) = \int_0^\infty q_\perp |J_{n,\ell,n,\ell'}(q_\perp R)|^2 dq_\perp$ ,  $J_{n,\ell,n,\ell'}(q_\perp R) = \frac{2}{R^2} \int_0^R \psi_{n',\ell'}(r) \exp(iq_\perp r) \psi_{n,\ell}(r) r dr$ , and  $\gamma = \sum_{n,\ell} e^{-\left(\frac{\hbar^2 B_{n,\ell}^2}{2m_e R^2 k_B T}\right)}$ .

### 3. Numerical Results and Discussion

In order to see clearly the characteristics of the absorption spectrum, we numerically evaluate the expression of absorption coefficient utilising specific parameters for the GaAs/AlAs quantum wire. The parameters used in the computation are taken from [8, 9].

In Fig. 1, we show the dependence of the absorption coefficient on the photon energy at the wire radius of  $R=16$  nm (dashed curve) and  $R=20$  nm (solid curve) with the temperature of 1 K. From the absorption spectrum, we can see the appearance of absorption maxima (peaks). The physical meaning of these peaks is easily deduced. For example, for the solid curve the left and the right peaks are located, respectively, at the photon energy of 35.3649 meV and 54.3388 meV and satisfy the following relations:

$$\hbar\omega = E_{0,2} - E_{0,1}; \quad (7)$$

$$\hbar\omega = E_{1,2} - E_{1,1}. \quad (8)$$

These relations describe the transitions of electron from the initial state  $(n, \ell) = (0,1)$  ( $(1,1)$ ) to the final state  $(n', \ell') = (0,2)$  ( $(1,2)$ ) by absorbing a photon with energy  $\hbar\omega$ . The case of  $R = 16$  nm (dashed curve) can be understood similarly. In general, we can conclude that the peaks satisfy the condition  $E_{n',\ell'} - E_{n,\ell} - \hbar\omega = 0$  which can be called optically detected electron - impurity resonance (ODEIR) condition. The ODEIR conditions give rise a possibility to determine experimentally the difference between energy subbands or the electron effective mass or the wire radius by using an optical field. For example, by measuring the photon energy at resonance  $\hbar\omega_{res}$ , one can obtain the separation between energy subbands  $\Delta E = E_{n',\ell'} - E_{n,\ell} = \frac{\hbar^2}{2m_e R^2} (B_{n',\ell'}^2 - B_{n,\ell}^2) = \hbar\omega_{res}$ . On the other hand, from the resonant photon energy one can also calculate the wire radius if the effective mass and the initial and final states are determined. The relation between the resonant photon energy and the quantum wire radius is shown in Fig. 2 for two typical transitions of electrons. One can see that as the wire radius increases, the resonant peaks shift to the smaller photon energy region (redshift). The redshift of the resonant peaks with increasing the confinement size of the systems has also been observed previously

in some low-dimensional materials such as quantum well [10], semiconductor superlattices [11], and quantum wires [8, 9].

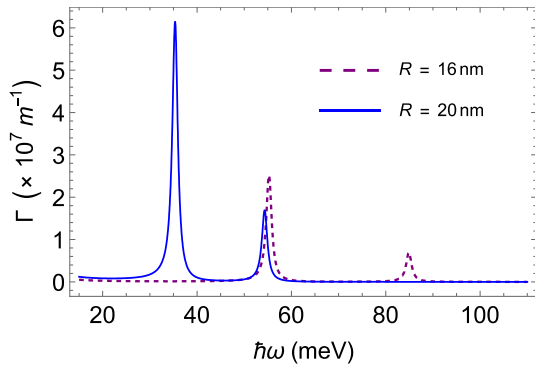


Figure 1. The absorption coefficient as a function of photon energy at different values of quantum wire's radius. Here,  $T = 1$  K.

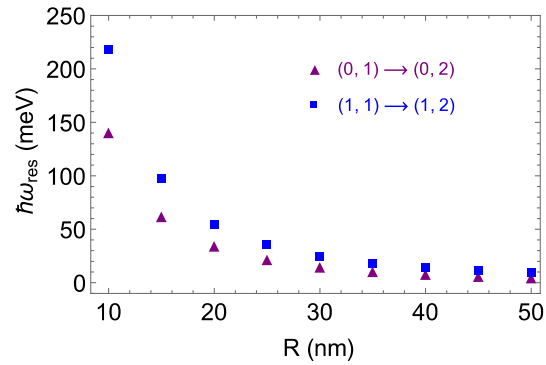


Figure 2. The relation between the resonant photon energy and quantum wire's radius for two different transitions. Here,  $T = 1$  K.

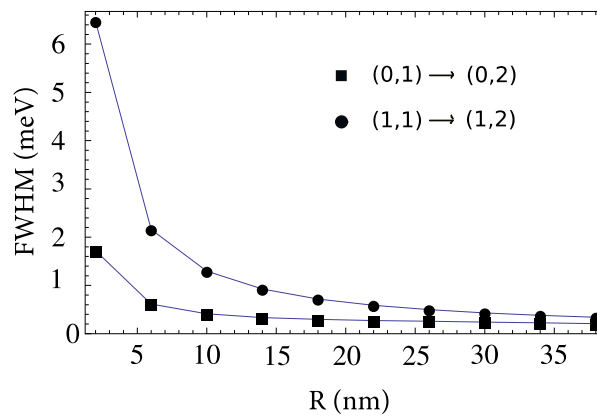


Figure 3. The FWHM as a function of quantum wire radius for two different transitions at temperature  $T = 1$  K.

Besides the position of the resonance peak, the full width at half maximum (FWHM) of the resonance peaks is also an important parameter when investigating the absorption spectrum. Therefore, we investigate the dependence of FWHM on the radius of wire. Using the profile method for determining FWHM [8-11], one obtain the FWHM of the absorption peaks at different values of the wire radius and show in Fig. 4 for the transition  $(0,1) \rightarrow (0,2)$  (filled squares) and the transition  $(1,1) \rightarrow (1,2)$  (filled circles). From the figure, one can see that FWHM decreases when the radius of the wire increases by the law  $FWHM = \exp(-aR^2 - bR + c)$  for both cases of transition with different constants  $a, b$  and  $c$ . The decrease of FWHM with increasing the confinement size is in accordance with previous calculated results in low-dimensional systems using other theories [8-13]. The decrease of the FWHM of the resonance peaks when increasing wire radius can be explained follows. As the radius of the quantum wire increases, the confinement effect is weakened, so the scattering probability of electrons and impurities is reduced. We also see from Fig. 3 that the FWHM for the transition  $(1,1) \rightarrow (1,2)$  change faster and have larger value than it does for the transition  $(0,1) \rightarrow (0,2)$ . Physically, the FWHM is proportional to the transition probability of electrons between states. The obtained result implies that the

transition probability for the transition  $(1,1) \rightarrow (1,2)$  is larger than it is for the transition  $(0,1) \rightarrow (0,2)$ . Mathematically, the values of the absorption coefficient and the FWHM are governed mainly by the transition matrix element given in Eq. (5). Moreover, the smaller the wire radius, the clearer the difference. By contrast, when the wire radius increases the difference between the two cases of transition becomes small and is identical at large radius. This behavior can be explained physically by the reduction confinement strength in the quantum wire when its radius is very large and the system then behaves like a bulk material, then the quantum numbers  $n$  and  $\ell$  does not play a role.

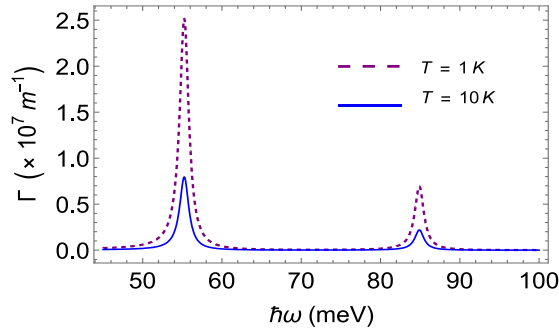


Figure 4. The absorption coefficient as a function of photon energy at different values of temperature. Here,  $R = 16$  nm.

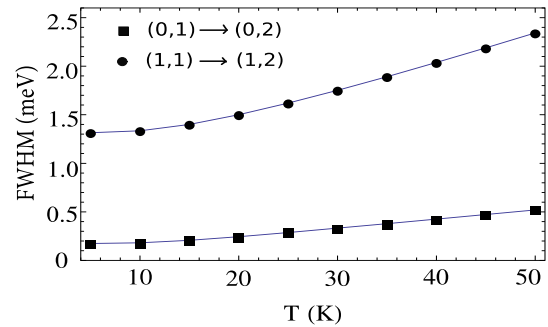


Figure 5. The FWHM as a function of temperature for 2 different transitions at radius  $R = 20$  nm.

The above ODEIR conditions do not depend on the temperature  $T$ , which means that the position of the resonance peaks remains unchanged as changing the temperature as illustrated in Fig. 4 where the plot of the absorption coefficient versus photon energy at two values of temperature is presented. From Fig. 4 one can see that only the height and the width of resonant peaks change as varying temperature. The effect of temperature on the FWHM is also investigated in detail. From the electron–impurity resonance conditions, we see that the resonance photon energy (position of resonance peak) does not depend on temperature  $T$ . That is why we have omitted through the temperature dependence of the electronic energy spectrum since these dependencies have been demonstrated in many materials is very weak that only care about the effect of temperature to FWHM. The dependence of the FWHM on temperature for the transition  $(0,1) \rightarrow (0,2)$  (filled squares) and the transition  $(1,1) \rightarrow (1,2)$  (filled circles) is shown in Fig. 5. It shows that FWHM increases in the range from 1 K to 50 K. This can be explained by the increase of the electron-impurity scattering probability as the temperature increases.

#### 4. Conclusion

We have theoretically investigated the optical absorption properties in a CQW taking account of the effect of electron - impurity interaction. Based on the general formula derived by the perturbation theory, we have calculated the optical absorption coefficient. The absorption spectra show ODEIR behaviour when the photon energy equals the separation between two electronic subbands. The ODEIR peaks show the redshift as the CQW's radius increases. By using the profile method, we have obtained computationally the FWHM of the ODEIR peaks. The FWHM decreases (increases) with increasing the CQW's radius (temperature). In particular, in the limit of large CQW's radius the contribution of transitions between electronic subbands to the absorption spectrum becomes identical, implying that the system tends to behave as a bulk (three-dimensional) system when the confinement length is large. The

above results can be seen as the basis for further studies and applications of low-dimensional materials in nano-optical electronic devices.

## Acknowledgments

This research is funded by Vietnam National Foundation for Science and Technology Development (NAFOSTED) under grant number 103.01-2020.61.

## References

- [1] H. Sakaki, Scattering Suppression and High-Mobility Effect of Size-quantized Electrons in Ultrafine Semiconductor Wire Structures. *Jpn. J. Appl. Phys.*, Vol. 19, 1980, pp. L735, <https://doi.org/10.1143/JJAP.19.L735>.
- [2] J. R. Soares, R. M. Almeida, L. G. Cançado, M. S. Dresselhaus, A. Jorio, Group Theory for Structural Analysis and Lattice Vibrations in Phosphorene Systems, *Phys. Rev. B*, Vol. 91, 2015, pp. 205421, <https://doi.org/10.1103/PhysRevB.91.205421>.
- [3] X. F. Wang, X. L. Lei, Polar-optic Phonons and High-Filed Electron Transport in Cylindrical GaAs/AlAs Quantum Wires, *Physical Review B*, Vol. 47, No. 7, 1994, pp. 4780, <https://doi.org/10.1103/PhysRevB.49.4780>.
- [4] H. V. Phuc, N. N. Hieu, Nonlinear Optical Absorption in Graphene Via Two-Photon Absorption Process, *Optics Communications*, Vol. 344, 2015, pp. 12-16, <https://doi.org/10.1016/j.optcom.2014.12.086>.
- [5] V. V. Karpunina, V. A. Margulis, Resonant Absorption of Electromagnetic Radiation in a Quantum Channel Due to the Scattering of Electrons by Impurities, *Optics and Spectroscopy*, Vol. 122, No. 6, 2017, pp. 979-983, <https://doi.org/10.1134/S0030400X17060108>.
- [6] V. V. Karpunin, V. A. Margulis, Resonance Absorption of Electromagnetic Radiation in a Phosphorene Single Layer, *Semiconductors*, Vol. 53, No. 4, 2019, pp. 458-464.
- [7] N. G. Galkin, V. A. Margulis, A. V. Shorokhov, Intraband Absorption of Electromagnetic Radiation by Quantum Nanostructures with Parabolic Confinement Potential, *Phys. Solid State*, Vol. 43, No. 3, 2001, pp. 530-538.
- [8] L. T. T. Phuong, H. V. Phuc, T. C. Phong, Influence of Phonon Confinement on the Optically-detected Electro-phonon Resonance Line-width in Cylindrical Quantum Wires, *Physica E*, Vol. 56, 2014, pp. 102-106, <http://dx.doi.org/10.1016/j.physe.2013.08.019>.
- [9] D. Q. Khoa, L. T. T. Phuong, B. D. Hoi, Nonlinear Absorption Coefficient and Optically Detected Electro-phonon Resonance in Cylindrical GaAs/AlAs Quantum Wires with Different Confined Phonon Models, *Superlattices and Microstructures*, Vol. 103, 2017, pp. 252-261, <https://doi.org/10.1016/j.spmi.2017.01.025>.
- [10] B. D. Hoi, L. T. T. Phuong, T. C. Phong, Optically Detected Electro-phonon Resonance in Quantum Wells Via Two-Photon Absorption Processes under the Influence of Phonon Confinement, *Superlattices and Microstructures*, Vol. 100, 2016, pp. 365-374.
- [11] N. T. Dung, V. T. T. Vi, L. T. T. Phuong, Nonlinear Optical Absorption and Optically Detected Electro-phonon Resonance in GaAs Based N-I-P-I Superlattices, *Micro and Nanostructures*, Vol. 165, 2022, pp. 207201, <https://doi.org/10.1016/j.micrna.2022.207201>.
- [12] H. Ham, H. N. Spector, Exciton Linewidth in Semiconducting Cylindrical Quantum Wire Structures Due to Scattering by Polar Optical Phonons: Finite Potential Well Model, *Journal of Applied Physics*, Vol. 90, 2001, pp. 2781, <https://doi.org/10.1063/1.1390492>.
- [13] H. Ham, H. N. Spector, Exciton Linewidth Due to Scattering by Polar Optical Phonons in Semiconducting Cylindrical Quantum Wire Structures, *Phys. Rev. B*, Vol. 62, 2000, pp. 13599, <https://doi.org/10.1103/PhysRevB.62.13599>.